

Self-collimation and focusing effects in zero-average index metamaterials

Rémi Pollès,* Emmanuel Centeno, Julien Arlandis, Antoine Moreau

LASMEA UMR-CNRS 6602 Université Clermont-Ferrand II, Campus des Cézeaux, 24,
Avenue des Landais, 63177 AUBIERE Cedex, France

*Remi.Polles@univ-bpclermont.fr

Abstract: One dimensional photonic crystals combining positive and negative index layers have shown to present a photonic band gap insensitive to the period scaling when the volume average index vanishes. Defect modes lying in this zero- \bar{n} gap can in addition be obtained without locally breaking the symmetry of the crystal lattice. In this work, index dispersion is shown to broaden the resonant frequencies creating then a conduction band lying inside the zero- \bar{n} gap. Self-collimation and focusing effects are in addition demonstrated in zero-average index metamaterials supporting defect modes. This beam shaping is explained in the framework of a beam propagation model by introducing an harmonic average index parameter.

© 2011 Optical Society of America

OCIS codes: (160.5293) Photonic bandgap materials; (160.3918) Metamaterials.

References and links

1. J. Joannopoulos, S. Johnson, D. Winn, and R. Meade, *Photonic crystals: molding the flow of light*, 2nd edition, (Princeton University Press 2008).
2. I. Nefedov and S. Tretyakov, "Photonic band gap structure containing metamaterial with negative permittivity and permeability," *Phys. Rev. E* **66**, 036611 (2002).
3. J. Li, L. Zhou, C. Chan, and P. Sheng, "Photonic band gap from a stack of positive and negative index materials," *Phys. Rev. Lett.* **90**, 83901 (2003).
4. D. Bria, B. Djafari-Rouhani, A. Akjouj, L. Dobrzynski, J. Vigneron, E. E. Boudouti, and A. Nougouoi, "Band structure and omnidirectional photonic band gap in lamellar structures with left-handed materials," *Phys. Rev. E* **69**, 066613 (2004).
5. Y. Yuan, L. Ran, J. Huangfu, H. Chen, L. Shen, and J. Kong, "Experimental verification of zero order bandgap in a layered stack of left-handed and right-handed materials," *Opt. Express* **14**, 2220–2227 (2006).
6. S. Kocaman, R. Chatterjee, N. Panoiu, J. Mcmillan, M. Yu, R. Osgood, D. Kwong, and C. Wong, "Observation of zeroth-order band gaps in negative-refraction photonic crystal superlattices at near-infrared frequencies," *Phys. Rev. Lett.* **102**, 203905 (2009).
7. V. Mocella, S. Cabrini, A. Chang, P. Dardano, L. Moretti, I. Rendina, D. Olynick, B. Harteneck, and S. Dhuey, "Self-collimation of light over millimeter-scale distance in a quasi-zero-average-index metamaterial," *Phys. Rev. Lett.* **102**, 133902 (2009).
8. N. Panoiu, J. Osgood, S. Zhang, and S. Brueck, "Zero-n bandgap in photonic crystal superlattices," *J. Opt. Soc. Am. B* **23**, 506–513 (2006).
9. I. Shadrivov, A. Sukhorukov, and Y. Kivshar, "Beam shaping by a periodic structure with negative refraction," *Appl. Phys. Lett.* **82**, 3820–3822 (2009).
10. F. Krayzel, R. Pollès, A. Moreau, and M. Mihailovic, "Simulation and analysis of exotic non-specular phenomena," *J. Europ. Opt. Soc. : Rap. Pub.* **5**, 10025 (2010).
11. E. Silvestre, R. Depine, M. Martínez-Ricci, and J. Monsoriu, "Role of dispersion on zero-average-index bandgaps," *J. Opt. Soc. Am. B* **26**, 581–586 (2009).
12. H. Kosaka, T. Kawashima, A. Tomita, M. Notomi, T. Tamamura, T. Sato, and S. Kawakami, "Self-collimating phenomena in photonic crystals," *Appl. Phys. Lett.* **74**, 1212–1214 (1999).
13. Throughout this paper, the inverse Fourier Transform is defined by $TF^{-1}(f(\alpha)) = \int_{-\infty}^{\infty} f(x) \exp(i\alpha x) d\alpha$.
14. M. Born, E. Wolf, and A. B. Bhatia, *Principles of optics: Electromagnetic theory of propagation, interference and diffraction of light* (Cambridge University press, Cambridge 2000).

1. Introduction

Photonic band gap materials have recently been revisited owing to the fascinating left-handed metamaterial properties. Bragg scattering in periodic positive index photonic crystals (PCs) is known to generate forbidden frequency bands for photons [1]. Although optical properties of photonic band gap devices are nowadays well known and used in many fields of photonic, a new kind of photonic crystal based on metamaterial properties have recently attracted significant attention. Photonic band gap metamaterials (PBGM) combining positive and negative index materials have shown to support a disallowed frequency band of intriguing properties [2],[3]. An omnidirectional photonic band gap, insensitive with respect to the period scaling, random or light polarization appears in one-dimensional PCs when the average optical index over the unit cell vanishes to zero [4]. This forbidden frequency band named zero- \bar{n} gap has been evidenced with stacked layers of metamaterials presenting both negative electric and magnetic permittivities in the GHz frequency range [5]. Similar experimental demonstrations have been led in near-infrared domain with the use of two-dimensional photonic crystal layers that emulate negative-index materials [6], [7]. Transmission pikes lying in the zero- \bar{n} gap have in addition been theoretically predicted when a resonant optical condition similar to Fabry-Perot (FP) condition is satisfied [3]. Although these resonant states have not yet been experimentally observed, they present unusual properties. Indeed, conversely to defect modes obtained in positive PCs devices, FP resonant states appears without introducing any lattice defects such as cavities in PBGMs and consequently they extend over the entire structure [8]. PBGMs have also proven interesting properties in terms of beam shaping [9] or self-collimation effect [7]. The latter has in particular been demonstrated with a specific device which can be viewed as a periodic set of flat lenses of -1 optical index alternated with air-layers. A Gaussian beam launched in this structure propagates without suffering of diffraction since the beam spreading in the air-layers is exactly cancelled by the focusing power of the PC-layers. Note that in this experiment the self-collimation regime is based on the excitation of propagating modes Bloch modes lying in the conduction band rather than FP resonant states lying in the zero- \bar{n} gap.

In this work, we first demonstrate that refractive index dispersion can open a transmission band instead of the theoretical narrow FP resonance in the zero- \bar{n} gap. This result, developed in section 2, points that an experimental demonstration of FP states requires an accurate control of metamaterial index dispersion. In section 3, we challenge to give the optical conditions necessary to get self-collimation and focusing effects in PBGM supporting FP resonant states. It is shown that these beam shaping properties arising in zero-average index materials are explained in terms of a harmonic average index condition.

2. Resonant modes in dispersive photonic band gap metamaterials

Consider a 1D PBGM consisting in a set of periodic layers of thickness d_1 and d_2 and optical indices n_1 and n_2 respectively. The PBGM's unit cell of period $D = d_1 + d_2$ combines right- and left-handed materials presenting either both positive electric and magnetic permittivities ϵ_1 and μ_1 or simultaneously negative permittivities ϵ_2 and μ_2 . The left-handed layers present then a negative optical index $n_2 = -\sqrt{\epsilon_2\mu_2}$. Infinite PBGMs are characterized by the following dispersion equation (1) where the Bloch wave propagation constant κ depends on the layer impedances $\eta_i = \sqrt{\mu_i/\epsilon_i}$ in the medium i and on the average index $\bar{n} = (n_1d_1 + n_2d_2)/D$ [3]:

$$\cos(\kappa D) = \cos(\bar{n}kD) + \frac{(\eta_1 - \eta_2)^2}{2\eta_1\eta_2} \sin(n_1kd_1) \sin(|n_2|kd_2), \quad (1)$$

here $k = 2\pi/\lambda$ is the wave number in vacuum. Providing that the impedances are mismatched ($\eta_1 \neq \eta_2$), the zero- \bar{n} gap opens when $\bar{n} = 0$ since no real propagation constant κ can be found.

However, allowed transmission pikes appear for singular wavelengths satisfying the following FP condition: $\Lambda_m = 2n_1d_1/m$ where m is a non-zero integer [3]. For a non-dispersive PBGM consisting of a finite number $N = 50$ of unit cells, sharp transmission pikes centered on these singular wavelengths are observed in the reflection diagram, see black curves of Fig. 1. The reflection coefficient of the finite size PC is computed for TM-polarized light with the rigorous electromagnetic code described in [10]. Similar results can be found in the TE polarization case.

Metamaterials are however dispersive so that $\bar{n} = 0$ is only satisfied for a particular wavelength. It has been shown that dispersion reduce the spectral bandwidth of the zero- \bar{n} gap in the off resonance regime [11]. Here, we would emphasis the impact on dispersion in opening FP resonances. For that purpose, optical index dispersion is only considered for the left-handed material. We choose $n_2(\lambda) = n_2^0 + \Delta n_2(\lambda)$, where $\Delta n_2(\lambda) = C(\lambda - \lambda_0)$ is assumed in first approximation to be a linear function vanishing at the wavelength λ_0 . The constant C is chosen to $0.5/\lambda_0$ which amounts to consider weakly dispersive left-handed layers. The zero-average index condition is then obtained at λ_0 when $n_1d_1 + n_2^0d_2 = 0$. The Taylor expansion of Eq. (1) in neighborhoods of the resonant wavelength gives us:

$$\cos(\kappa D) \simeq 1 + \Gamma x_m^2 + \Gamma \Delta n_2(\lambda) k d_2 x_m - (\Delta n_2(\lambda) k d_2)^2 / 2, \quad (2)$$

where $x_m = n_2(\lambda) k d_1 - m\pi$ and $\Gamma = (\eta_1 - \eta_2)^2 / (2\eta_1\eta_2)$. Equation (2) shows that when $|\cos(\kappa D)| \leq 1$, bands of transmission centered on the resonances are found instead of the discrete sharp pikes. The spectral width of such bands, derived from Eq. (2), increases with the index mismatch seen around the m th resonance:

$$\Delta_m \lambda = \frac{mA(\eta_2^2 - \eta_1^2)(\lambda_0 - \Lambda_m)}{A^2\eta_2\eta_1 - m(A+m)(\eta_2 - \eta_1)^2}, \quad (3)$$

where $A = 2d_2C$. These results are illustrated with a PBGM presenting a zero-average index condition exactly satisfied at the reduced frequency $D/\lambda_0 = 13/8$ (so that $\Delta n_2(\lambda_0) = 0$). As

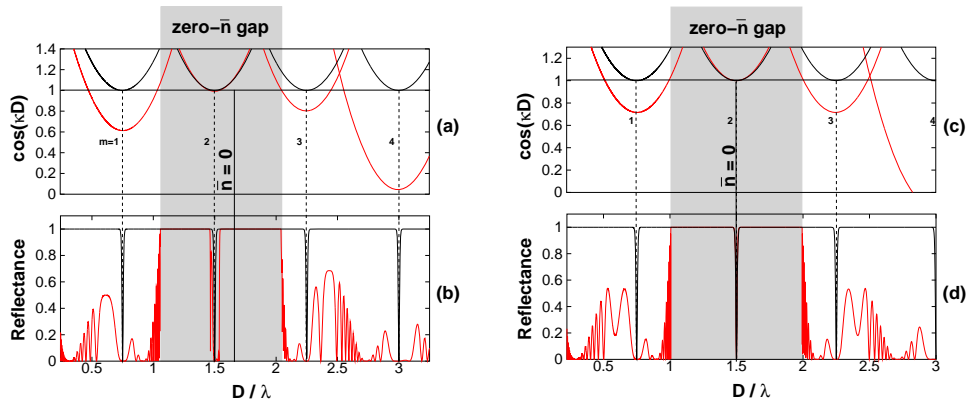


Fig. 1. (a) and (c): dispersion relation given by Eq. (1) (black curve) and its Taylor expansions (Eq. (2)) (red curve). (b) and (d): reflectance of the structure composed of $N = 50$ periods. Black curves correspond to the nondispersive case and red curves to the dispersive case. (a) and (b): the structure is characterized by $n_1 = 1$, $n_2^0 = -2$, $\eta_1 = 1$, $\eta_2 = 0.5$, $d_1 = 2D/3$, $d_2 = D/3$ and $D/\lambda_0 = 13/8$ (which corresponds to $D = 1.625\lambda_0$). (c) and (d): the parameters are the same but $D/\lambda_0 = 3/2$.

shown in Fig. 1a, FP modes are affected by index dispersion and the singular allowed wavelengths Λ_m are now replaced by bands of transmission (red curves). Since index dispersion

prevents exactly fulfill the FP condition, the transmission pikes broaden when the spectral distance $|\lambda_0 - \Lambda_m|$ increases, Fig. 1b. The first and the third resonances become in this scheme large conducting bands whose upper and lower boundaries determine the zero- \bar{n} gap edges. The reflection spectrum also indicates that a large conduction band opens between the third and the fourth resonances. Note that the Taylor expansion of Eq. (2) around the resonances is valid at the vicinity of $\bar{n} = 0$. This explains why this Taylor expansion cannot strictly match with the reflection diagram outside the zero- \bar{n} gap. However, inside the zero- \bar{n} gap, the tiny transmission band is recognized as the second order FP resonance. For higher optical dispersion, this second order FP band could even overlap the conduction band preventing then a clear interpretation of the transmission diagram.

The impact of dispersion is nevertheless limited if the second order FP mode is centered on λ_0 because the numerator of Eq. (3) vanishes when $\Lambda_2 = \lambda_0$. A sharp pike appears in this case obtained by tuning the reduce frequency to $D/\lambda_0 = 3/2$ and by keeping fixed the other optical parameters, Fig. 1c and 1d. Finally, the observation of a sharp transmission pike in the zero- \bar{n} gap requires to simultaneously satisfies $\bar{n} = 0$ and FP resonance conditions. This may be a challenge in dispersive PGBM since it amounts to precisely control the optical thicknesses of the left- and right-handed layers.

3. Self-collimation and focusing effects in zero-average index materials

Recent experimental results reporting the propagation of sub-wavelength self-collimated beams over several millimeters have shown a new type of beam shaping principle [7]. Self-collimation originally discovered in positive index 2D photonic crystal is understood thanks to the analysis of photonic surface dispersion [12]. When flat iso-frequency curves are considered, all the Bloch waves forming the beam are propagated with parallel group velocities. If this analysis applies for photonic conduction bands, it is not suitable for defect modes lying in photonic band gaps. FP modes in the zero- \bar{n} gap are in particular delocalized modes spreading in the entire structures and are consequently characterized by a singular frequency and a discrete couple set of Bloch wavevectors. These specific properties prevent the use of the classical dispersion surface analysis for predicting the beam propagation dynamic in PBGM supporting FP states. We address this problem by considering a model based on a beam propagation theory and we demonstrate beam shaping properties in zero-average index materials. For that purpose, the second FP modes is considered and index dispersion is controlled by fixing $\Lambda_2 = \lambda_0$. Since transmission almost attains 100%, only forward waves need to be considered and reflections at the layers interfaces are neglected. An incident Gaussian beam $U^i(x, y = 0) = \exp(-(x/W_0)^2)$ of waist W_0 and centered on the first layer at $y = 0$ is launched inside the crystal consisting in N periods. This beam can also be represented by the following Fourier integral: $U^i(x, y) = \int_{-\infty}^{\infty} U^i(\alpha) \exp(i\beta(\alpha)y) \exp(i\alpha x) d\alpha$, α and β being the propagation constants in the x - and y -direction respectively with $\beta = \sqrt{(\omega n_1/c)^2 - \alpha^2}$. To derive an analytical formulation of the beam at the output interface $y = L$ (with $L = ND$), the electromagnetic field is expressed as the inverse Fourier integral [13] of the product of the incident field Fourier transform with the phase propagator operators of each layers [14] :

$$U(x, L) = TF^{-1} \{ U^i(\alpha) (P_1(\alpha, d_1) P_2(\alpha, d_2))^N \}. \quad (4)$$

Here $U^i(\alpha) = (W_0/(2\sqrt{\pi})) \exp(-(\alpha W_0/2)^2)$ and the phase propagator in the layer of optical index n_i is $P_i(\alpha, y) = \exp(i\beta_i(\alpha)y)$ where $\beta_i = \sqrt{(\omega n_i/c)^2 - \alpha^2}$ with $i = 1, 2$. When $\alpha \ll \frac{\omega}{c} n_i$, the paraxial assumption holds and the phase propagator becomes $P_i(\alpha, y) = \exp(iy(\frac{\omega}{c} n_i - \frac{\alpha^2}{2n_i \omega}))$. Plugging this expression in Eq. (4) gives:

$$U(x, L) = TF^{-1} \{ U^i(\alpha) \tilde{P}(\alpha, D)^N \}. \quad (5)$$

Here $\tilde{P}(\alpha, y) = \exp(iy(\frac{\omega}{c}\bar{n} - \frac{\alpha^2}{2}\frac{c}{\omega}\langle\frac{1}{n}\rangle))$ is the average phase operator expressed in terms of average index \bar{n} and harmonic average index $\langle\frac{1}{n}\rangle = \frac{1}{D}\int_0^D\frac{dx}{n(x)}$ over the crystal period. It is worth noticing that the PBGM can be seen as an equivalent medium provided that the two kinds of average optical indices are considered. Equation (5) allows us to derive the expression of the beam at the PBGM exit:

$$U(x, L) = \frac{W_0}{\bar{\omega}(L)} e^{-\left(\frac{x}{\bar{\omega}(L)}\right)^2} e^{i\frac{\omega}{c}\langle n \rangle L} e^{i\varphi(x, L)}, \quad (6)$$

where the complex functions $\bar{\omega}(L)$ and $\varphi(x, L)$ are given by: $\bar{\omega}(L) = (W_0^2 + 2iL\langle\frac{1}{n}\rangle)^{1/2}$ and $\varphi(x, L) = \langle\frac{1}{n}\rangle 2x^2L/|\bar{\omega}(L)|^2$. It is seen that the waist of the beam at $L = ND$ takes almost a common form:

$$W(L) = W_0 \sqrt{1 + \theta_0^2 (ND)^2 \left\langle \frac{1}{n} \right\rangle^2}, \quad (7)$$

$\theta_0 = \lambda/(\pi W_0^2)$ being the diverging angle. However, conversely to positive index photonic crystal, PBGMs enable to cancel the harmonic average index $\langle\frac{1}{n}\rangle$. Therefore when $\langle\frac{1}{n}\rangle = 0$, the beam is refocused after each unit cell and exits the device with its initial waist W_0 . Finally, self-collimation effect for FP modes lying in zero- \bar{n} gap occurs when:

$$\frac{d_1}{n_1} + \frac{d_2}{n_2} = 0. \quad (8)$$

This additional optical condition combined with the zero average index one $\bar{n} = 0$ implies that the layers thicknesses are equal and that opposite refraction indices are considered, i.e. $d_1 = d_2$ and $n_1 = -n_2$. We note that these conditions, $\langle\frac{1}{n}\rangle = 0$ and $\bar{n} = 0$, can be achieved when $\eta_1 \neq \eta_2$. This proves that zero-average index materials supporting FP modes can propel self-collimated beams. This case is illustrated with a PBGM supporting a second order FP mode in the zero- \bar{n} gap, Fig. 2a. Self-collimation is observed throughout 200 unit cell for an incident Gaussian beam of waist $W_0 = 5\lambda$. Another consequence of using FP resonances is the exact phase compensation of the propagated field along the PBGM. Equation (7) actually shows that when $\langle\frac{1}{n}\rangle = 0$ and $\bar{n} = 0$, the outgoing beam is exactly identical to the incident beam: $U(x, L) = U^i(x, 0)$. The incident beam is then translated through the PBGM without suffering from phase difference and beam spreading.

Remark that in V. Mocella's and co-authors experimental demonstration, self-collimation has been achieved with propagating Bloch modes instead of FP modes lying in the zero- \bar{n} gap [7]. Indeed, the reported sub-wavelength self-collimation mechanism has been obtained by almost matching the layer impedances ($\eta_1 \simeq \eta_2$) i.e. when the zero- \bar{n} gap is expected to nearly close. However, in this experiment, the optical parameters were chosen to satisfy Eq. (8), showing that this optical condition also applies outside the zero- \bar{n} gap.

Let us now demonstrate focalization properties in zero-average index materials. Consider a PBGM embedded in a homogenous medium of index n_0 and illuminated with an incident Gaussian beam shifted away from the input interface by a distance f . For sketch of simplicity the exterior medium is air so that $n_0 = 1$. The beam computed at a distance f' of the exit layer is obtained by applying the propagator operator $P_0(\alpha, y)$ to the beam in the object and image planes. Equation (5) now becomes:

$$U(x, L) = TF^{-1} \{ U^i(\alpha) P_0(\alpha, f) \tilde{P}(\alpha, D)^N P_0(\alpha, f') \}, \quad (9)$$

where $P_0(\alpha, y) = \exp(iy(\frac{\omega}{c}n_0 - \frac{\alpha^2}{2n_0}\frac{c}{\omega}))$. By solving Eq. (9) one can derive the waist at the image distance:

$$W(f') = W_0 \sqrt{1 + \theta_0^2 \left(\frac{f}{n_0} + ND \left\langle \frac{1}{n} \right\rangle + \frac{f'}{n_0} \right)^2}. \quad (10)$$

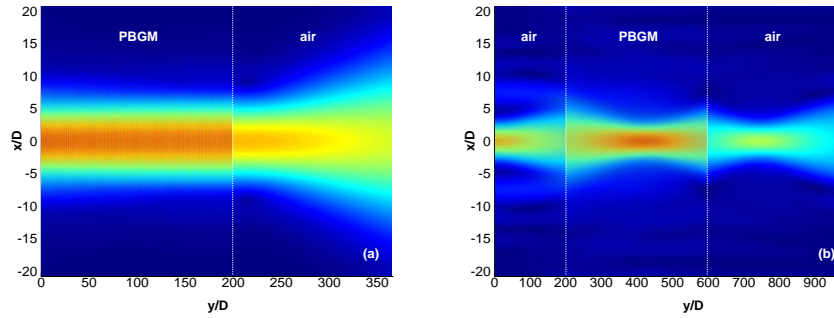


Fig. 2. Modulus of the field when a PBGM, embedded in a air-medium ($n_0 = 1$), is illuminated by a beam. (a) The parameters of the PBGM are $N = 200$, $d_1 = d_2 = D/2$, $n_1 = 2$, $n_2^0 = -2$, $\eta_1 = 1$, $\eta_2 = 0.5$ and $D = \lambda_0$. (b) The parameters of the PBGM are $N = 400$, $d_1 = D/3$, $d_2 = 2D/3$, $n_1 = 1$, $n_2^0 = -0.5$, $\eta_1 = 1$, $\eta_2 = 0.5$ and $D = 3\lambda_0$.

The beam is then focused when $W(f') = W_0$, i.e. if the foci satisfy the following optical condition:

$$f + f' = -ND \left\langle \frac{1}{n} \right\rangle n_0. \quad (11)$$

This condition shows that PBGMs behave as a flat lens when the harmonic average index $\left\langle \frac{1}{n} \right\rangle$ is negative even when the average index \bar{n} is kept to zero. A -1 harmonic average index can in particular be obtained for a low metamaterial optical index value of $n_2^0 = -0.5$ when the following parameters are chosen: $n_1 = -2n_2$ and $d_2 = 2d_1$. This focusing property is demonstrated with the second order FP mode obtained at the reduce frequency $D/\lambda_0 = 3$ and for an incident Gaussian beam presenting a waist $W_0 = 10\lambda_0$, Fig. 2b. In accordance to Eq. (11), a symmetric image of the incident beam is formed when $f = f' = ND/2$. Despite evanescent waves are not relied over the structure, the full width at half maximum (FWHM) of the exit beam attains $1.06W_0$ showing an excellent focalization power of PBGM even after hundred of wavelengths. Remark that these beam shaping are obtained when the impedance mismatch between two consecutive layers is weak. When larger impedance mismatch is considered, the quality of these optical effects decreases since backwards waves interfere more strongly with forward waves.

4. Conclusion

We have shown that index dispersion plays in crucial role for obtaining resonance states in zero-average index 1D photonic crystals. It is demonstrated that an allowed band appears in the zero- \bar{n} gap instead of a sharp pike when the FP resonance condition is not exactly satisfied. Self-collimation and focusing effects have been next demonstrated in PBGM supporting FP states lying in the zero- \bar{n} gap. These beam shaping properties are understood by introducing a harmonic average index parameter. Despite the null average index condition holds, self-collimation or focalization are obtained when the harmonic average index is either null or negative. Up to date, PBGMs are unique optical devices which present a resonant self-collimation effect inside a photonic band gap.

Acknowledgements

This work was supported by the Agence Nationale pour la Recherche of France (NT09_517025). The authors thank the Centre Informatique National de l'Enseignement Supérieur for its computing support.